



Numerical Simulation of Projectile Acceleration Process Using Solid/Gas Two-Phase Reacting Flow Model

Hiroaki MIURA¹, Akiko MATSUO¹ and Yuichi NAKAMURA²

¹Department of Mechanical Engineering, Keio University, JAPAN

²NOF Corporation, JAPAN

Systems Utilizing Solid Propellant

Chemical energy of
solid propellant
 $\approx 4\text{MJ/kg}$



Kinetic energy of
projectile

Gun System

Military Technology
Cannon

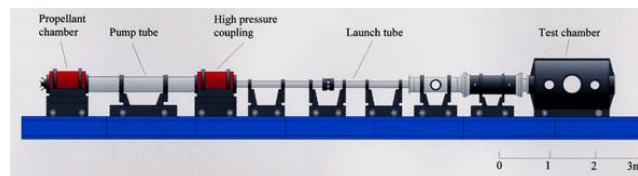


<http://www.army-technology.com/projects/crusader/crusader5.html>

Scientific Research
Ballistic Range



<http://www.knlab.msl.titech.ac.jp/>



<http://ceres.ifs.tohoku.ac.jp/~coe/facility.html>

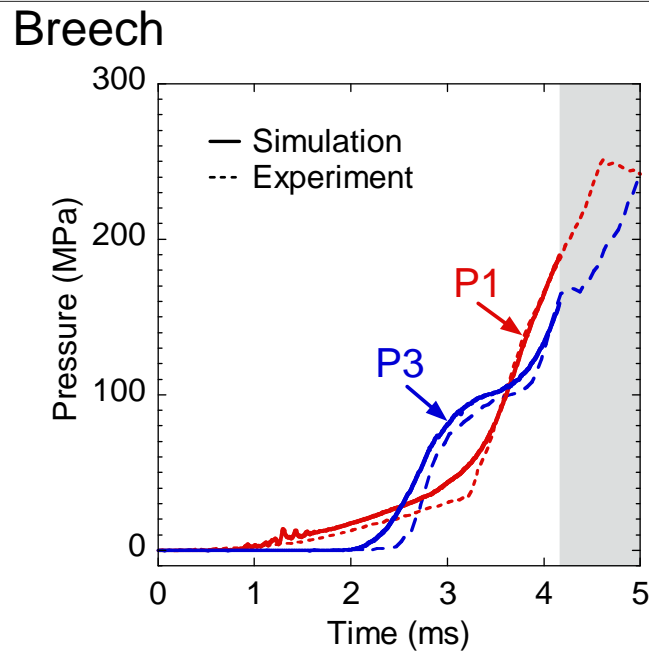
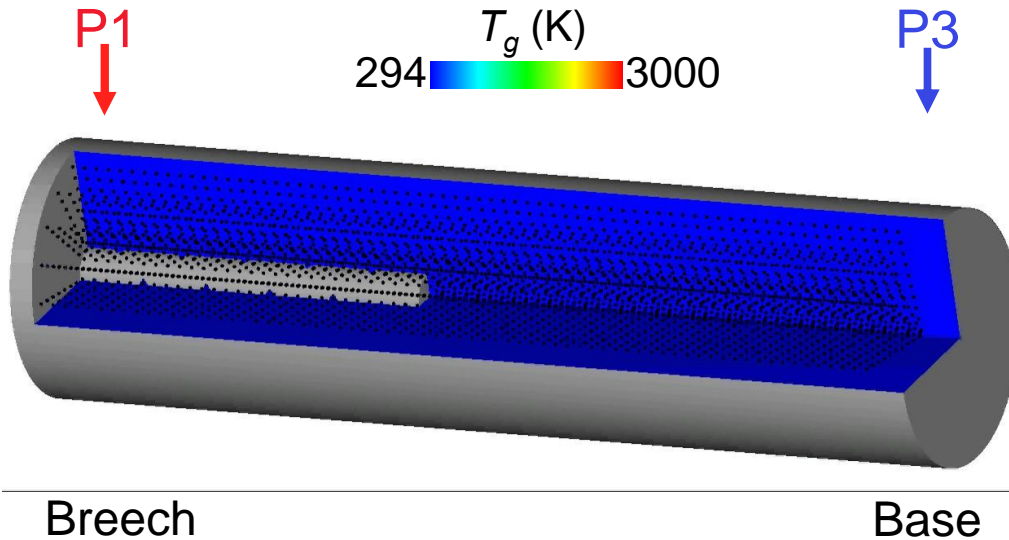
Solid Rocket

Space Propulsion
Solid Rocket Booster



http://spaceinfo.jaxa.jp/db/kaihatu/shuttle/shuttle_g/sts-87-2.jpg

Pressure of Granular Solid Propellant



H. Miura *et al.*, ISEM2008

The movement of granular solid propellant causes the chamber pressure fluctuations.



Simulation of propellant grains movement is significant to predict the destructive pressure waves generation.

bular Solid Propellant

Granular propellant



Characteristics of granular propellant

- “ Larger surface area
Rapid fire
- “ Easy adjustment
for propellant mass
- “ Problem of strong
pressure waves



Tubular propellant



Characteristics of tubular propellant

- “ Smaller surface area
Slow burning
- “ Uniform ignition and
uniform charge
concentration

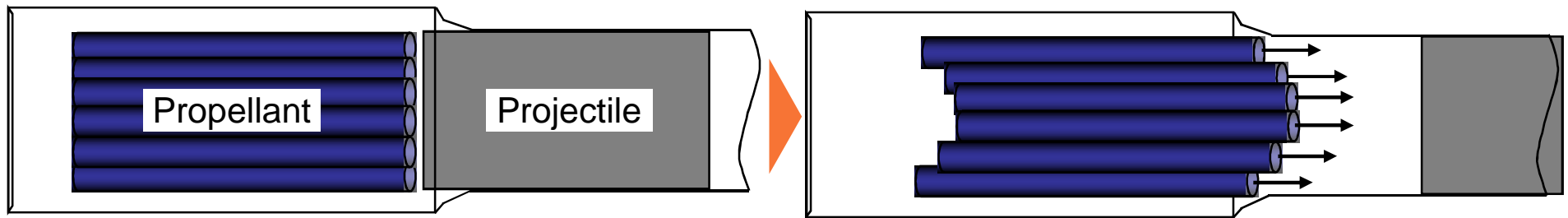
FAS Military Analysis Network

Simulation technique for tubular propellant combustion should be developed.

Modeling for tubular propellant movement with burning

n of Tubular Solid Propellant

To simulate tubular propellant behavior in the chamber



Modeling for tubular propellant movement with burning

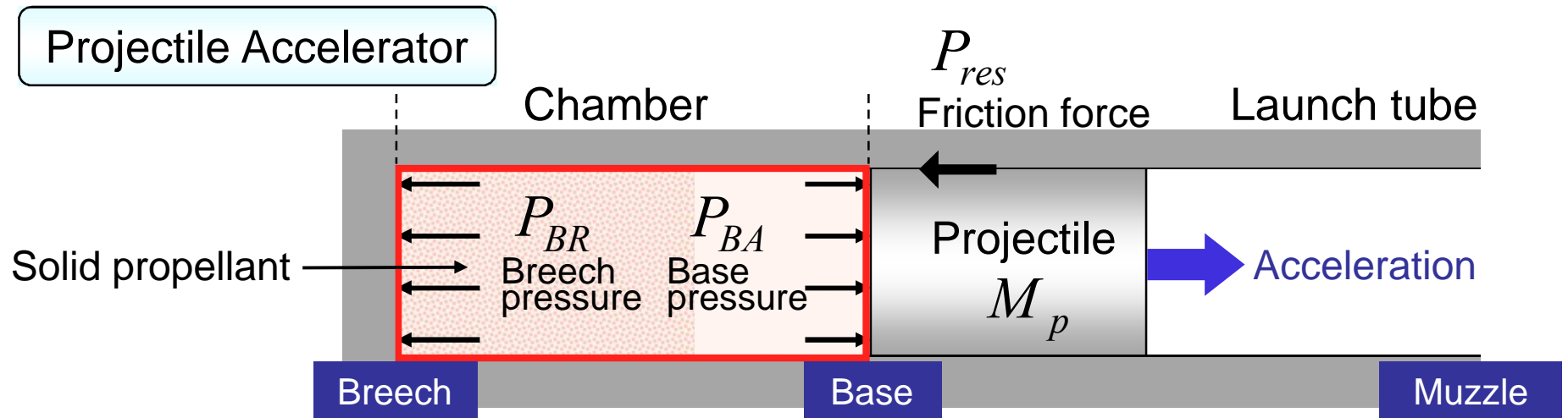
- ❑ A long tubular propellant lies in the wide range of computational domain.

Consideration of property distributions on propellant surface

- ❑ Each tubular propellant moves in the chamber.

Movement model for propellants by Lagrangian approach

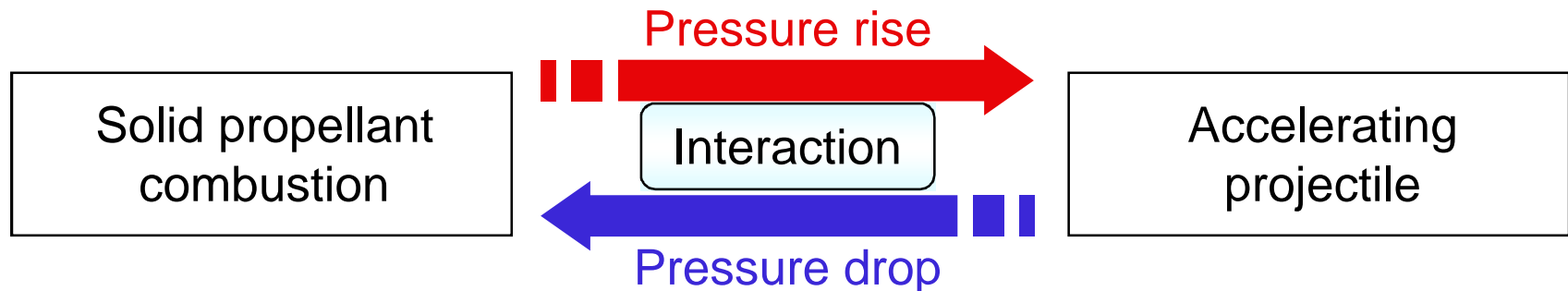
Model for Projectile Accelerator



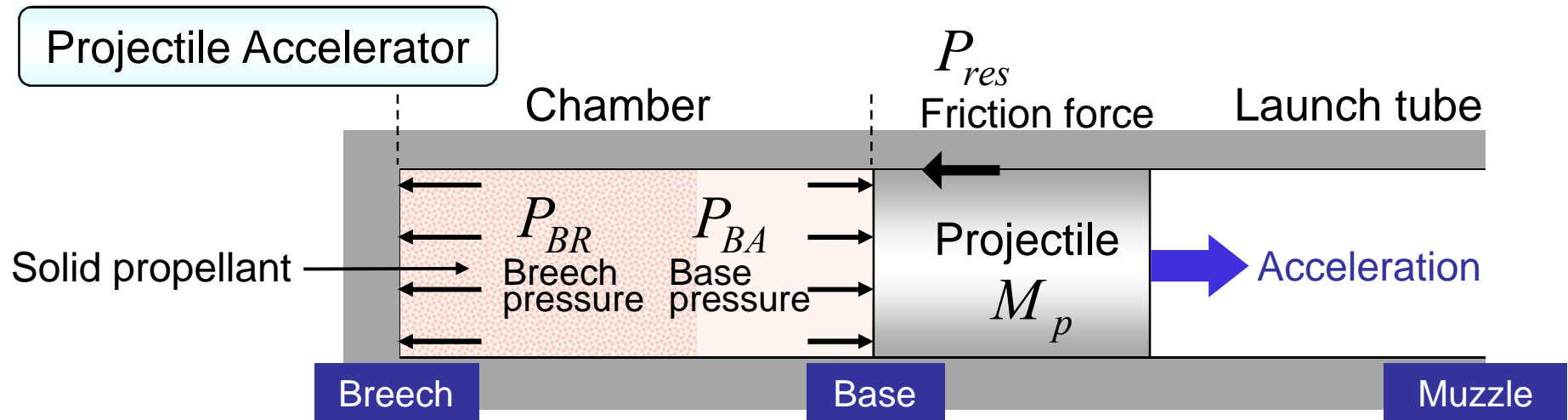
- ❑ Combustion gas and solid propellant coexist in the chamber.



- ❑ Chamber volume increases with the projectile movement.




Analysis Based on Interior Ballistics



Prediction of events in the accelerator is required.

Elements of accelerating process simulation by numerical analysis

- ☐ Solid/Gas two-phase flow
- ☐ Solid propellant combustion
 - Propellant (Solid phase)  Combustion gas (Gas phase)
- ☐ Moving boundary problem

Objective

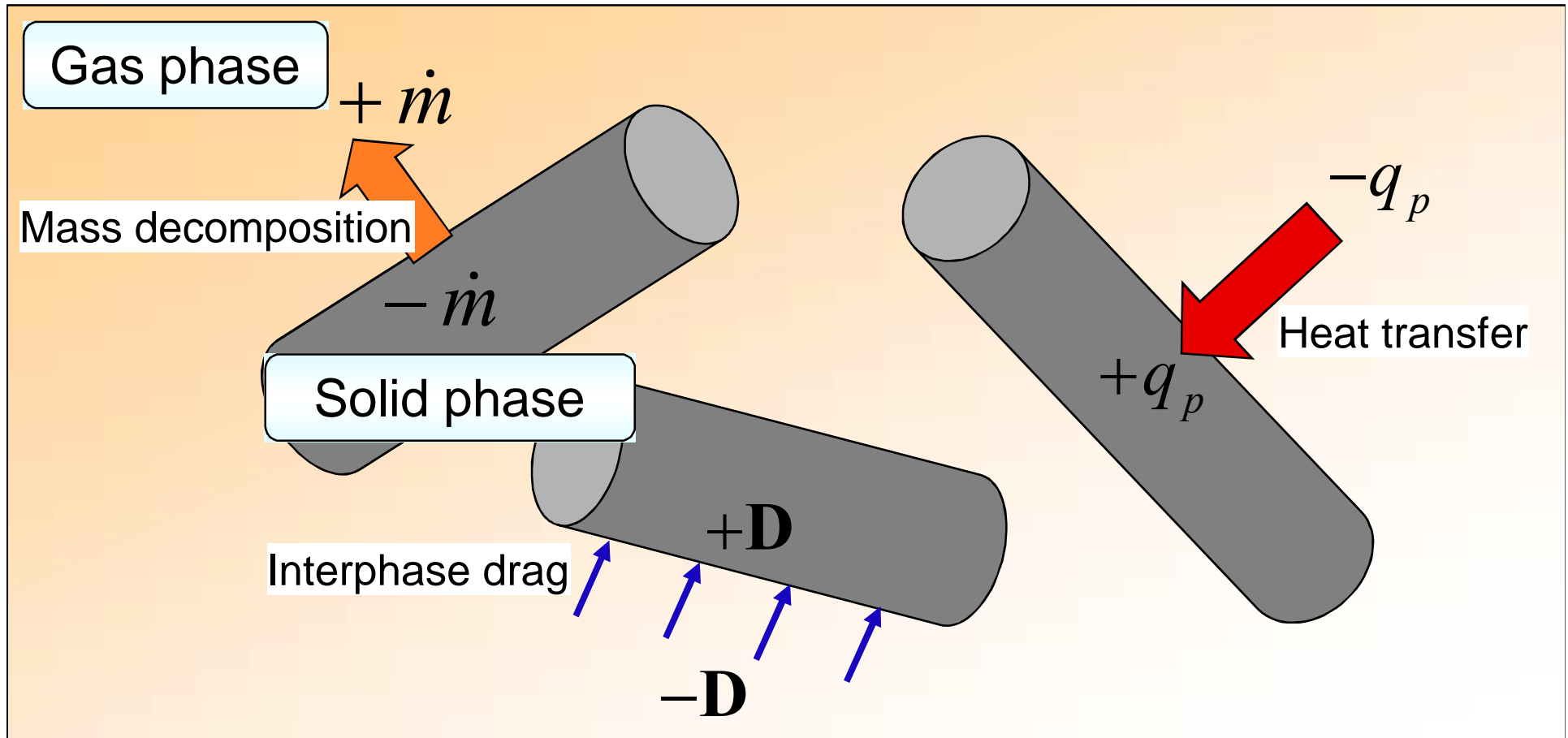
To simulate the process of accelerating a projectile by tubular solid propellant combustion in the 50mm projectile accelerator using the developed 2D axisymmetric two-phase flow code and the moving overlapped grid method.

- Simulation method is validated using experimental data.
 - “ Breech pressure history
 - “ Projectile velocity history
- Conditions of projectile mass M_p and propellant mass C are varied for the examination of those effects on the performance of gun system.
 - “ Maximum breech pressure
 - “ Projectile muzzle velocity and kinetic energy

Calculation Method for Interior Ballistics Simulation

- Two-phase Fluid Dynamics Code
- Modeling Tubular Propellant
- Modeling Projectile Movement

Interaction Between Two Phases



$$\dot{m} = \dot{m}(r) \quad r = ap^n$$

$$\mathbf{D} = \mathbf{D}(\mathbf{u}_g - \mathbf{u}_p)$$

$$q_p = q_p(T_g - T_p)$$

$$T_p \geq T_{\text{ignition}} \rightarrow \text{ignition}$$

Governing Equations

Gas-phase

$$\frac{\partial}{\partial t}(\underline{\alpha\rho}) + \nabla \cdot (\underline{\alpha\rho\mathbf{u}}) = \dot{m} + \dot{m}_{ig}$$

$$\frac{\partial}{\partial t}(\underline{\alpha\rho\mathbf{u}}) + \nabla \cdot (\underline{\alpha\rho\mathbf{u}\mathbf{u}}) = -\underline{\alpha}\nabla p - \mathbf{D} + \dot{m}\mathbf{u}_p$$

$$\frac{\partial}{\partial t}(\underline{\alpha e}) + \nabla \cdot \{\underline{\alpha}(e + p)\mathbf{u}\} = -\mathbf{D} \cdot \mathbf{u}_p + \dot{m}\left(q + \frac{\mathbf{u}_p \cdot \mathbf{u}_p}{2}\right) + \dot{m}_{ig}q_{ig} - q_p$$

$$\begin{cases} \frac{\partial}{\partial t}(\alpha\rho Y_{pr}) + \nabla \cdot (\alpha\rho Y_{pr}\mathbf{u}) = \dot{m} \\ \frac{\partial}{\partial t}(\alpha\rho Y_{ig}) + \nabla \cdot (\alpha\rho Y_{ig}\mathbf{u}) = \dot{m}_{ig} \\ \frac{\partial}{\partial t}(\alpha\rho Y_a) + \nabla \cdot (\alpha\rho Y_a\mathbf{u}) = 0 \end{cases}$$

pr : propellant gas
 ig : igniter gas
 a : air

Solid-phase

$$m_{p,i} \frac{du_{p,i}}{dt} = (p_L - p_R)A_i + D_i - \dot{m}_i u_{p,i}$$

1D motion of i -th propellant

{ **Gas-phase** **Compressible fluid**
 Solid-phase **Constant density**

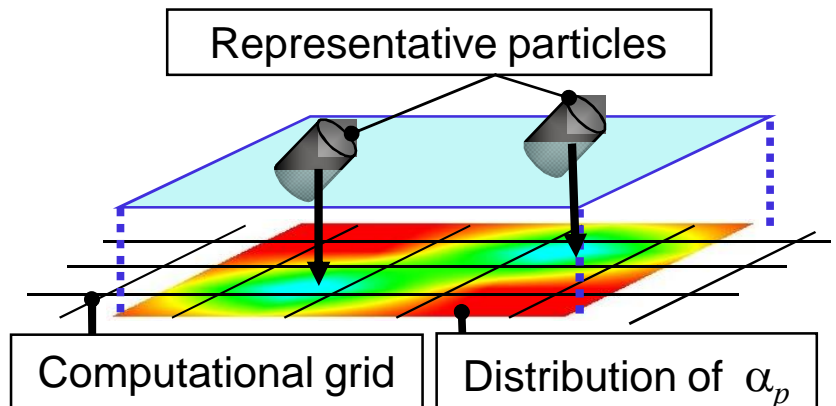
Computational volume is divided into the volume of gas and solid.

α : Volume fraction of gas-phase (porosity)

α_p : Volume fraction of solid-phase

$$\alpha = 1 - \alpha_p$$

The distribution of α_p is determined from the distribution of representative particles.



Governing Equations

$$\begin{aligned}
 \text{Gas-phase} \quad & \frac{\partial}{\partial t}(\alpha \rho) + \nabla \cdot (\alpha \rho \mathbf{u}) = \dot{m} + \dot{m}_{ig} \\
 & \frac{\partial}{\partial t}(\alpha \rho \mathbf{u}) + \nabla \cdot (\alpha \rho \mathbf{u} \mathbf{u}) = -\alpha \nabla p - \mathbf{D} + \dot{m} \mathbf{u}_p \\
 & \frac{\partial}{\partial t}(\alpha e) + \nabla \cdot \{\alpha (e + p) \mathbf{u}\} = -\mathbf{D} \cdot \mathbf{u}_p + \dot{m} \left(q + \frac{\mathbf{u}_p \cdot \mathbf{u}_p}{2} \right) + \dot{m}_{ig} q_{ig} - q_p
 \end{aligned}
 \quad
 \begin{cases}
 \frac{\partial}{\partial t}(\alpha \rho Y_{pr}) + \nabla \cdot (\alpha \rho Y_{pr} \mathbf{u}) = \dot{m} \\
 \frac{\partial}{\partial t}(\alpha \rho Y_{ig}) + \nabla \cdot (\alpha \rho Y_{ig} \mathbf{u}) = \dot{m}_{ig} \\
 \frac{\partial}{\partial t}(\alpha \rho Y_a) + \nabla \cdot (\alpha \rho Y_a \mathbf{u}) = 0
 \end{cases}$$

pr : propellant gas
 ig : igniter gas
 a : air

$$\text{Solid-phase} \quad m_{p,i} \frac{du_{p,i}}{dt} = (p_L - p_R) A_i + D_i - \dot{m}_i u_{p,i} \quad \text{1D motion of } i\text{-th propellant}$$

□ Gas-phase components

- Propellant combustion gas (pr)
- Igniter combustion gas (ig)
- Air (a)

□ State equation for gas-phase

$$p = \frac{RT}{(1/\rho - b)} \quad b : \text{Covolume}$$

\dot{m} : Propellant mass decomposition rate

\dot{m}_{ig} : Igniter mass decomposition rate

\mathbf{D} : The interphase drag between two-phase

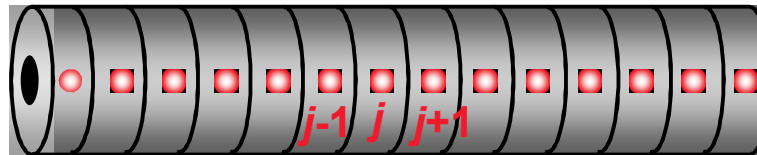
q : The combustion heat of propellant

q_{ig} : The combustion heat of igniter

q_p : Heat loss to solid phase

Representative Particle Properties

Information of propellant geometry for ***j*-th representative particle**



Representative particle

At the end of each tubular propellant

$$\text{Volume } V_{p,j} = (\Delta L_{p,j} - \Delta u_j) \left\{ \frac{\pi}{4} (D_p - 2\Delta u_j)^2 - \frac{\pi}{4} (d_p + 2\Delta u_j)^2 \right\}$$

$$\begin{aligned} \text{Surface area } S_{p,j} = & \pi (D_p - 2\Delta u_j) (\Delta L_p - \Delta u_j) + \pi (d_p + 2\Delta u_j) (\Delta L_{p,j} - \Delta u_j) \\ & + \left\{ \frac{\pi}{4} (D_p - 2\Delta u_j)^2 - \frac{\pi}{4} (d_p + 2\Delta u_j)^2 \right\} \end{aligned}$$

$\Delta L_{p,j}$: Divided length of tube

D_p : Outer diameter of tube

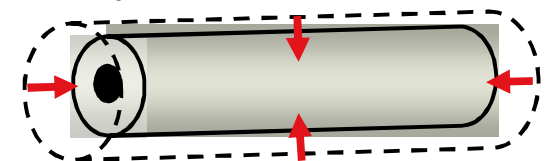
d_p : Inner diameter of tube

$$\Delta u_j = \int_0^t r dt \quad r = ap^n$$

At the other position

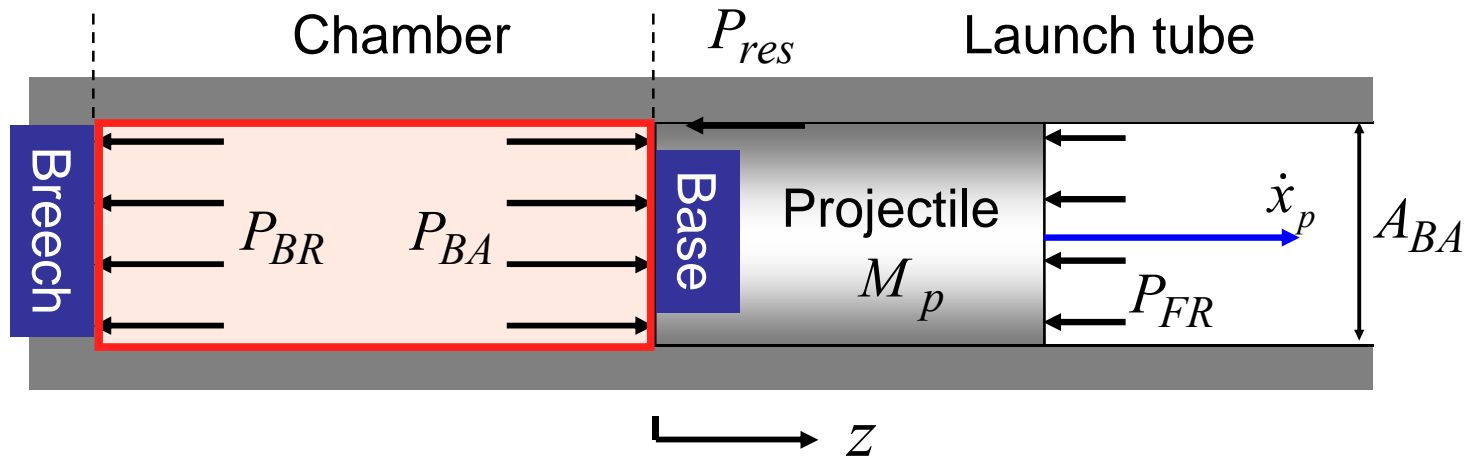
$$\text{Volume } V_{p,j} = \Delta L_{p,j} \left\{ \frac{\pi}{4} (D_p - 2\Delta u_j)^2 - \frac{\pi}{4} (d_p + 2\Delta u_j)^2 \right\}$$

$$\text{Surface area } S_{p,j} = \pi (D_p - 2\Delta u_j) \Delta L_p + \pi (d_p + 2\Delta u_j) \Delta L_{p,j}$$



Projectile Movement in Launch Tube

Kinetic model of projectile movement



P_{BR} : Breech pressure
 P_{BA} : Base pressure

P_{res} : Resistive pressure

Projectile velocity $\dot{x}_p = \int_0^t \ddot{x}_p dt = \int_0^t \left(\frac{(P_{BA} - P_{FR} - P_{res}) A_{BA}}{M_p} \right) dt$



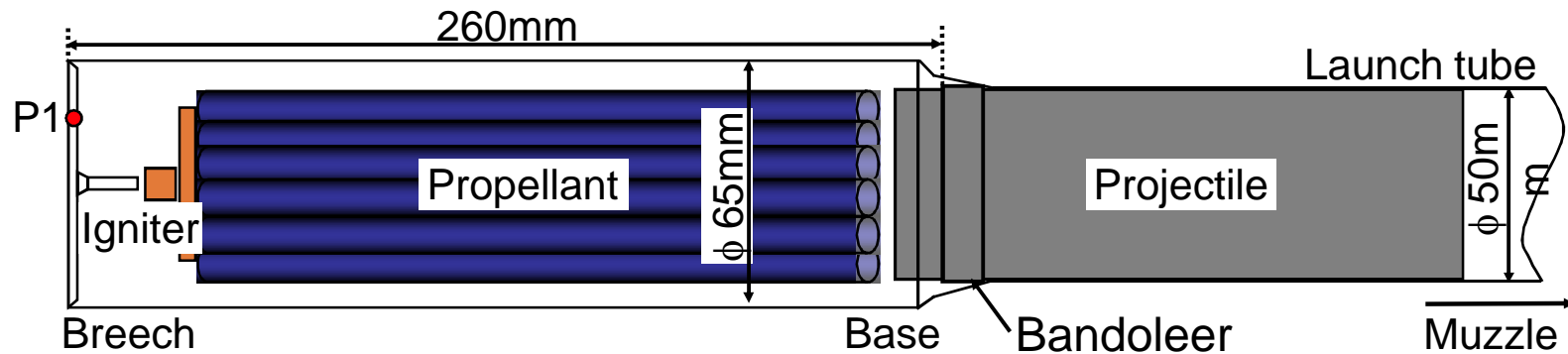
*Your complimentary
use period has ended.
Thank you for using
PDF Complete.*

[Click Here to upgrade to
Unlimited Pages and Expanded Features](#)

Interior Ballistics Simulation of 50mm Gun

Computational Model

Reproduction of the experiment of 50mm gun by NOF Corporation



The projectile velocity was recorded using an in-bore Doppler radar system.

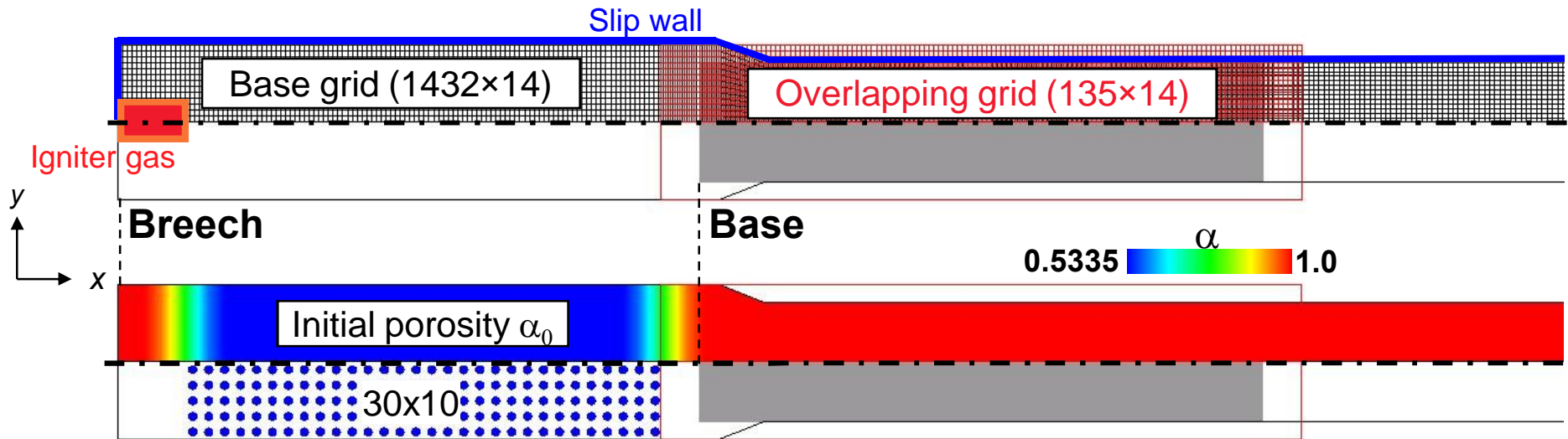
Computational data

Diameter of tube (mm)	50
Length of tube (mm)	3195
Projectile mass M_p (kg)	2.5, 3.5, 4.5
Propellant mass C (kg)	0.4, 0.5
Propellant type	Double-base
Shape of grain	Tubular (one hole)
Size of grain (mm)	$\phi 6.35 \times 200$

Propellant properties

Adiabatic flame temperature T_0 (K)	3133
Impetus F (J/g)	1036
Specific heat ratio γ	1.232
Density ρ_p (kg/m ³)	1615
Covolume b (cm ³ /kg)	993

Computational Setup



Calculation condition

Overlapping grid is movable

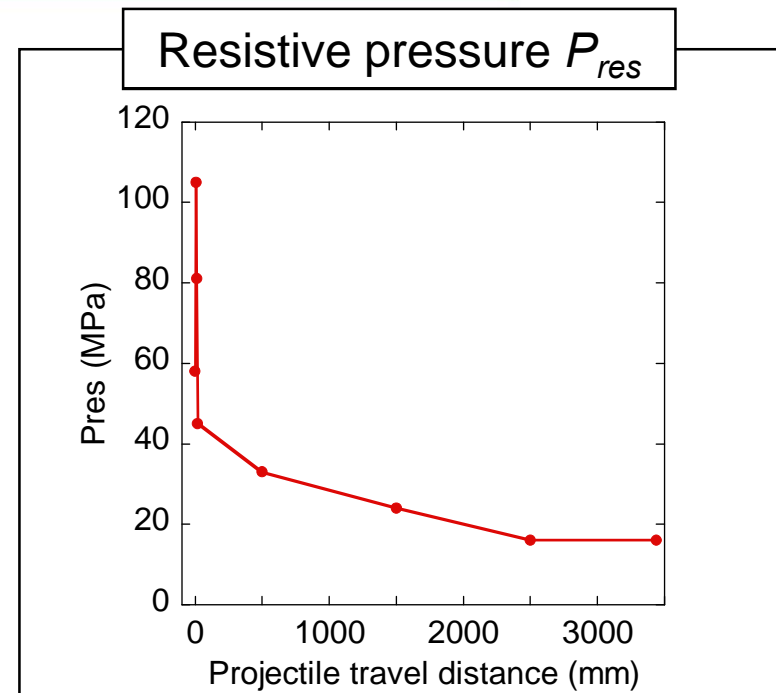
Wall condition : Adiabatic slip wall

Initial condition : 101kPa, 294K, $\gamma=1.4$

Calculation method

Discretization method of convection term
 : SHUS (Shima and Jounouchi, 1995)

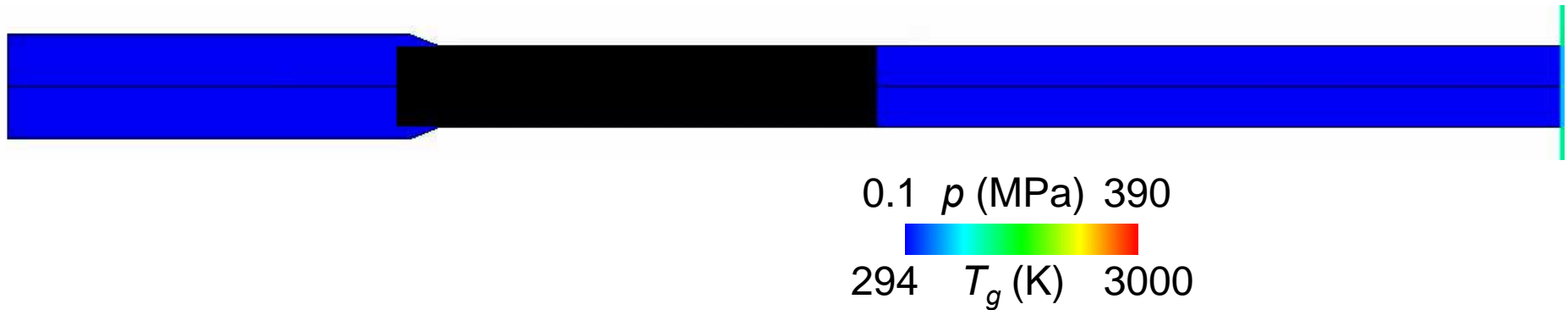
Time integration method
 : 2-step Runge-Kutta method



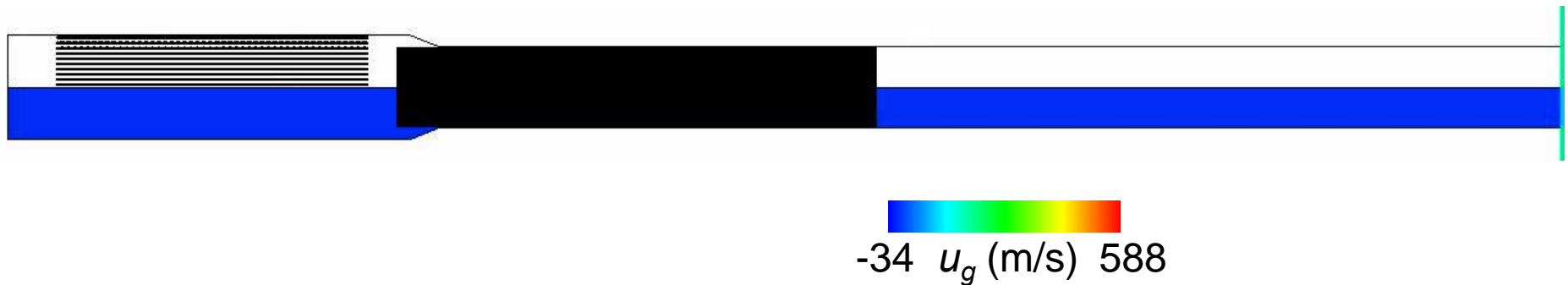
Accelerating Process

$$M_p = 4.5\text{kg and } C = 0.5\text{kg}$$

Pressure / gas temperature distribution

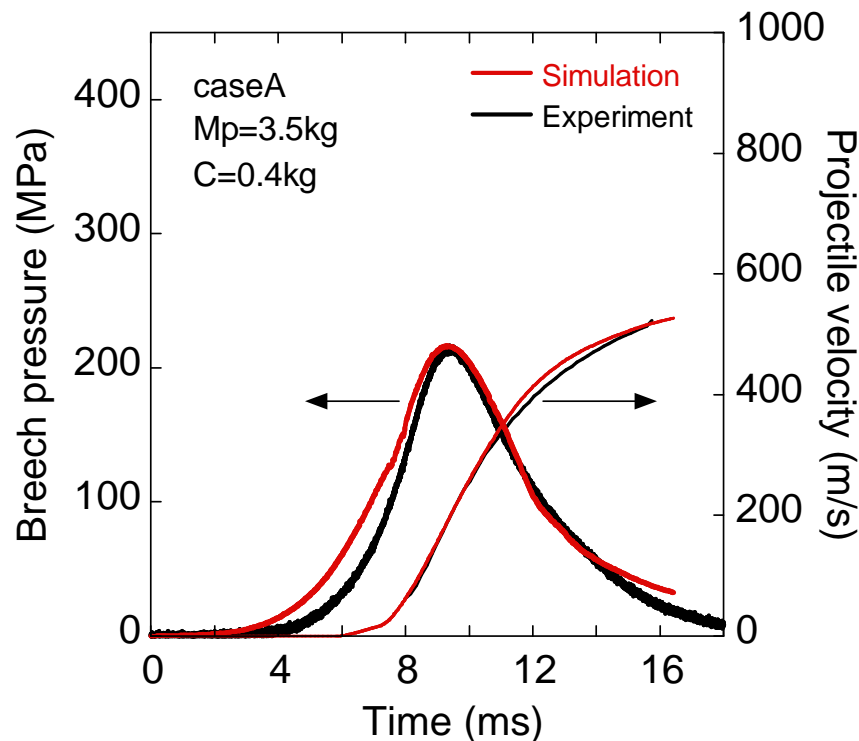


Propellant / gas velocity distribution

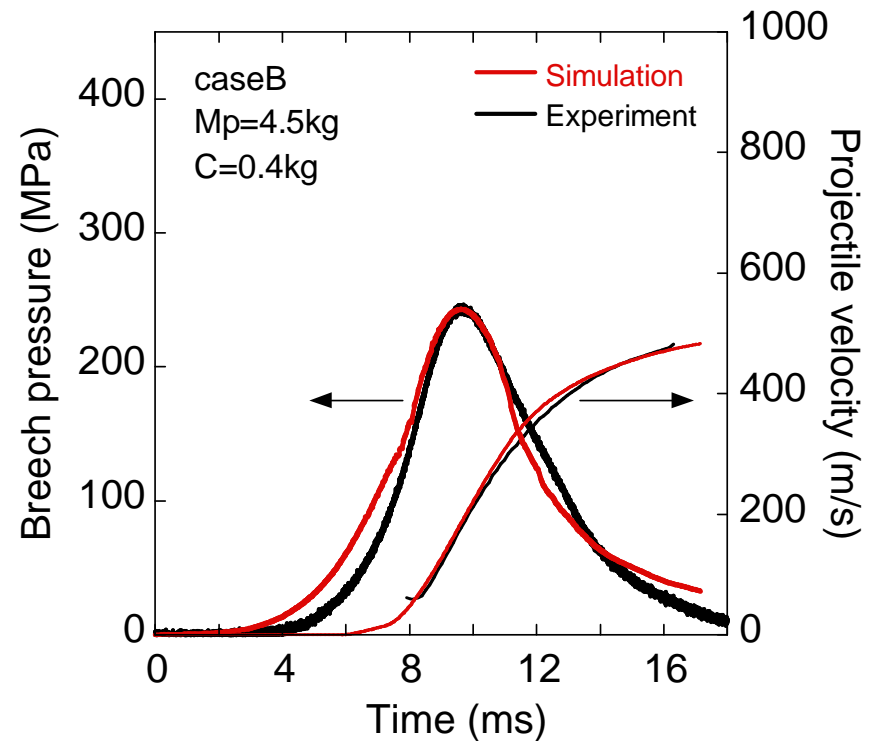


Comparison of Predicted Data with Experiment

Case A ($M_p=3.5\text{kg}$ and $C=0.4\text{kg}$)



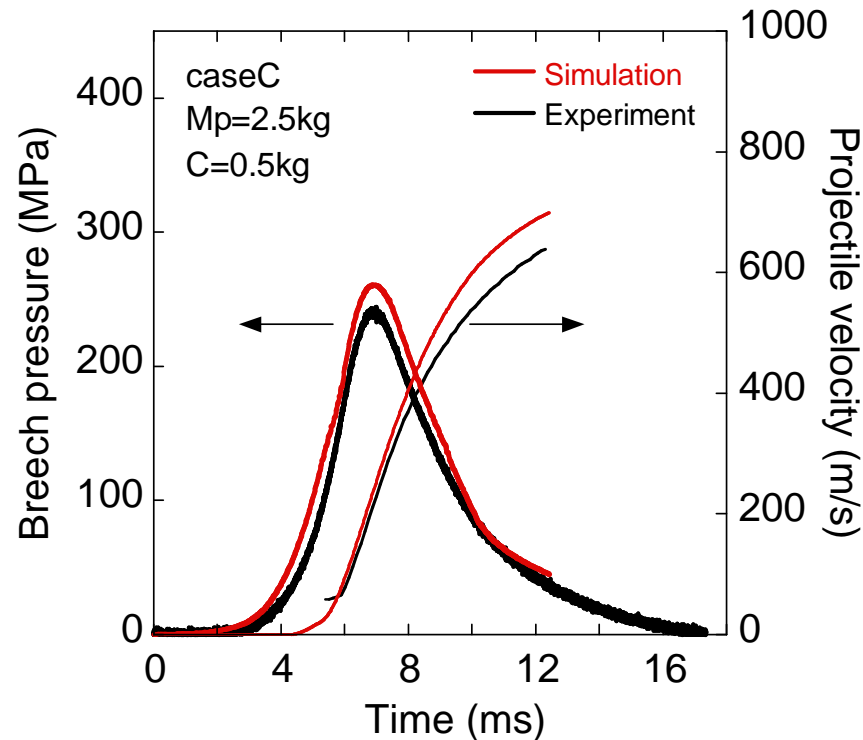
Case B ($M_p=4.5\text{kg}$ and $C=0.4\text{kg}$)



- ❑ Predicted histories of the breech pressure and the projectile velocity are in good agreement with the experimental data in the each case.

Comparison of Predicted Data with Experiment

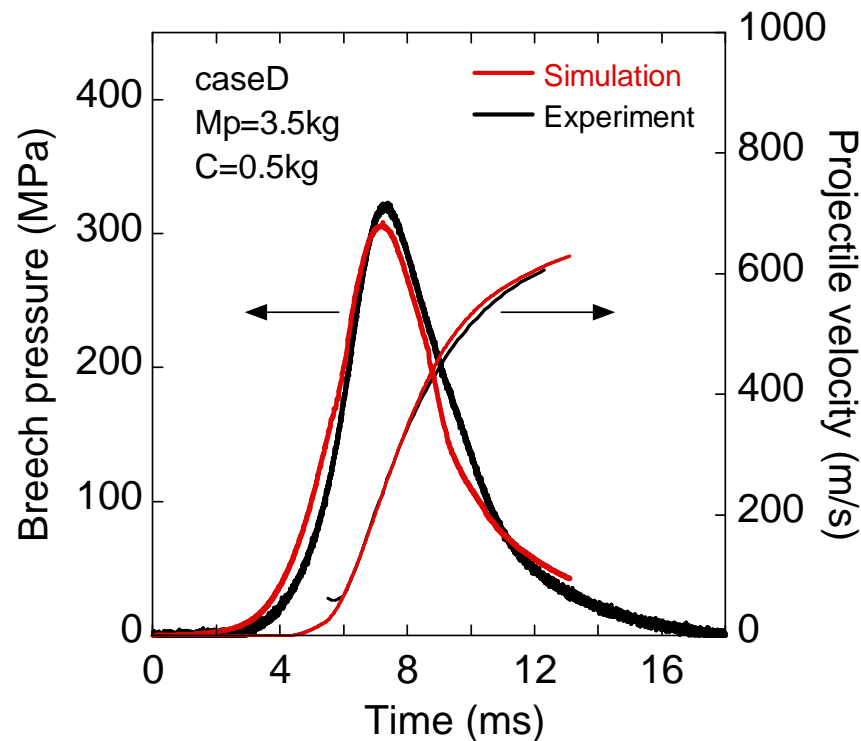
Case C ($M_p=2.5\text{kg}$ and $C=0.5\text{kg}$)



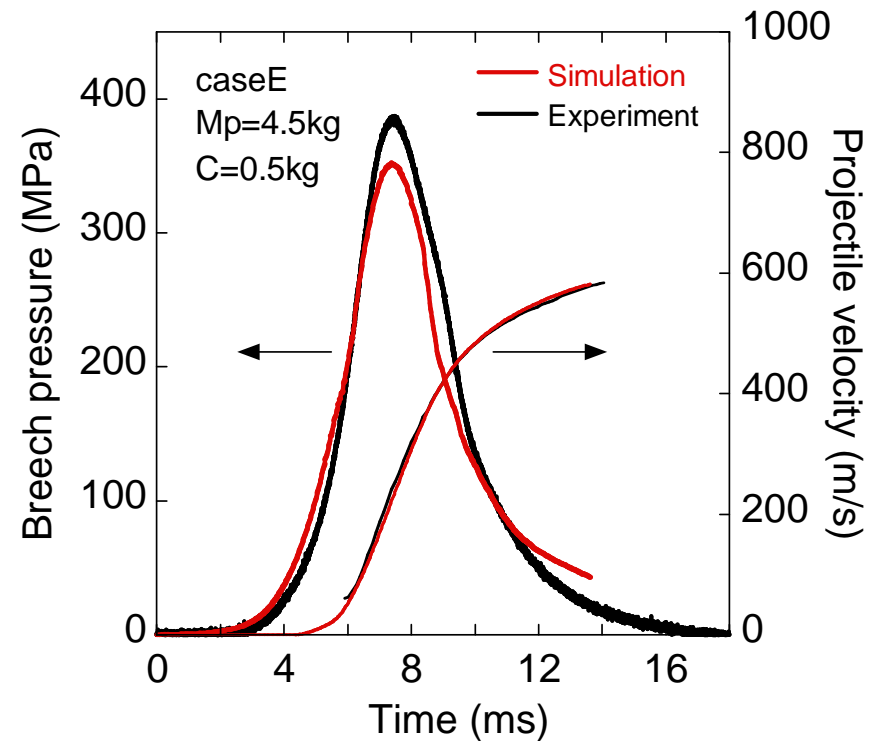
- ❑ Predicted breech pressure and projectile velocity are higher than the experimental data in this case.

Comparison of Predicted Data with Experiment

Case D ($M_p=3.5\text{kg}$ and $C=0.5\text{kg}$)



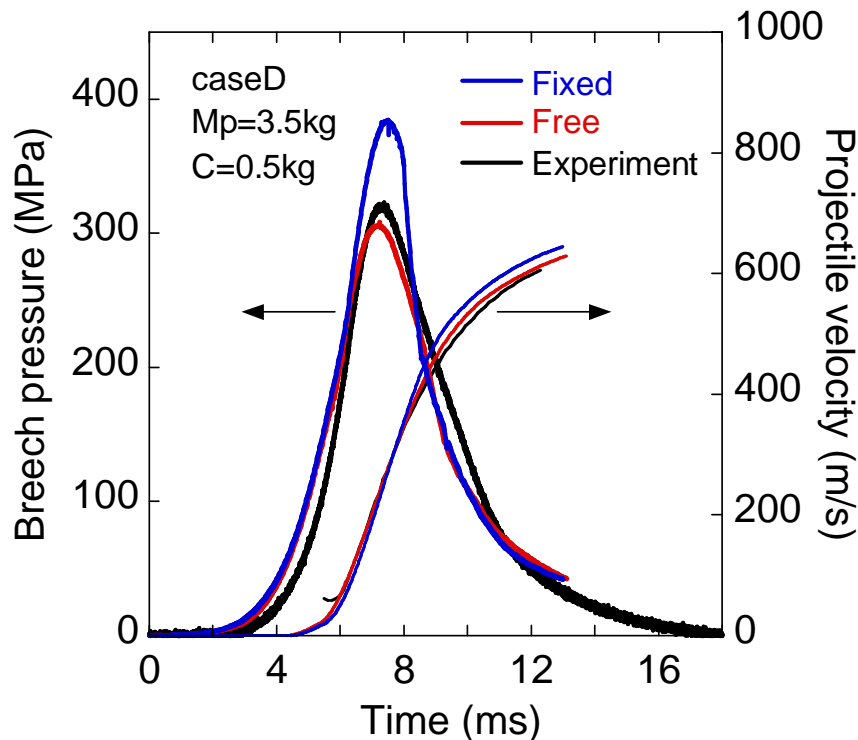
Case E ($M_p=4.5\text{kg}$ and $C=0.5\text{kg}$)



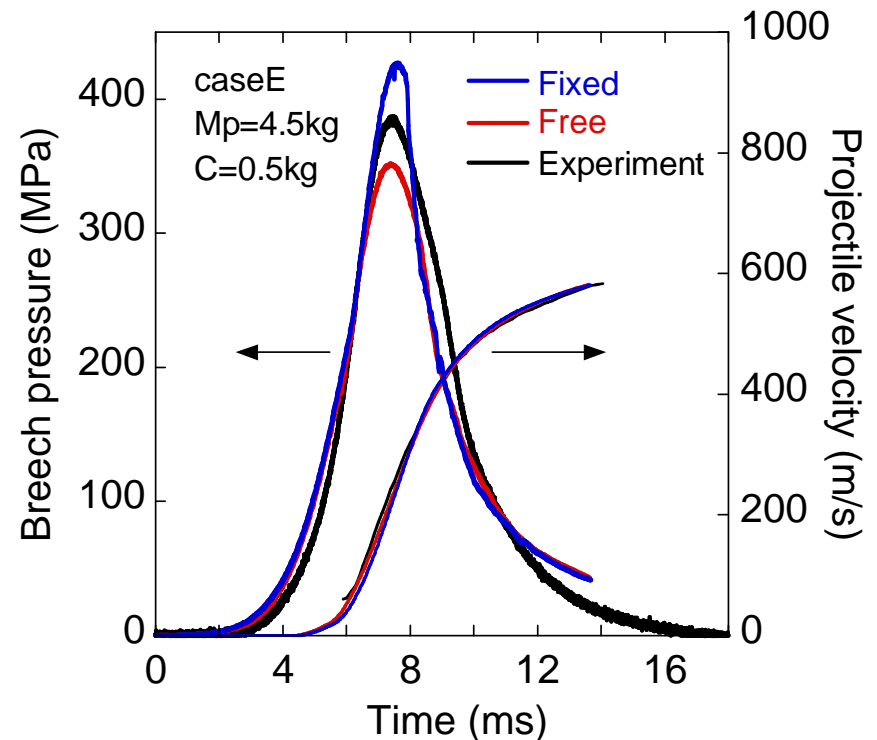
- ❑ Predicted histories of the breech pressure and the projectile velocity are in good agreement with the experimental data in the each case.

and Fixed Propellant Models

Case D ($M_p=3.5\text{kg}$ and $C=0.5\text{kg}$)



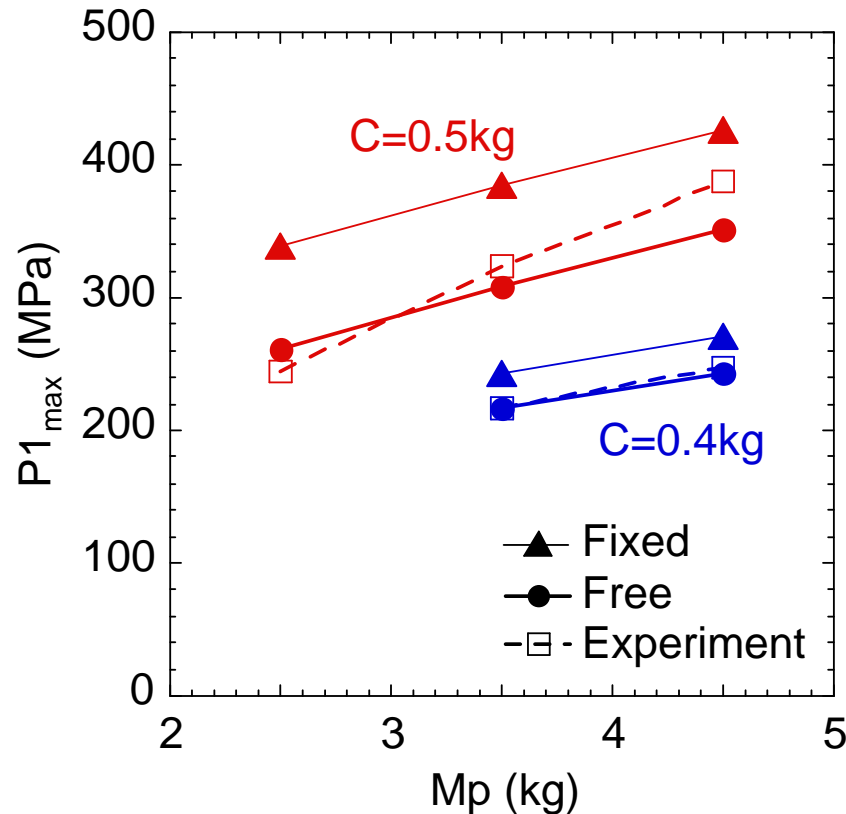
Case E ($M_p=4.5\text{kg}$ and $C=0.5\text{kg}$)



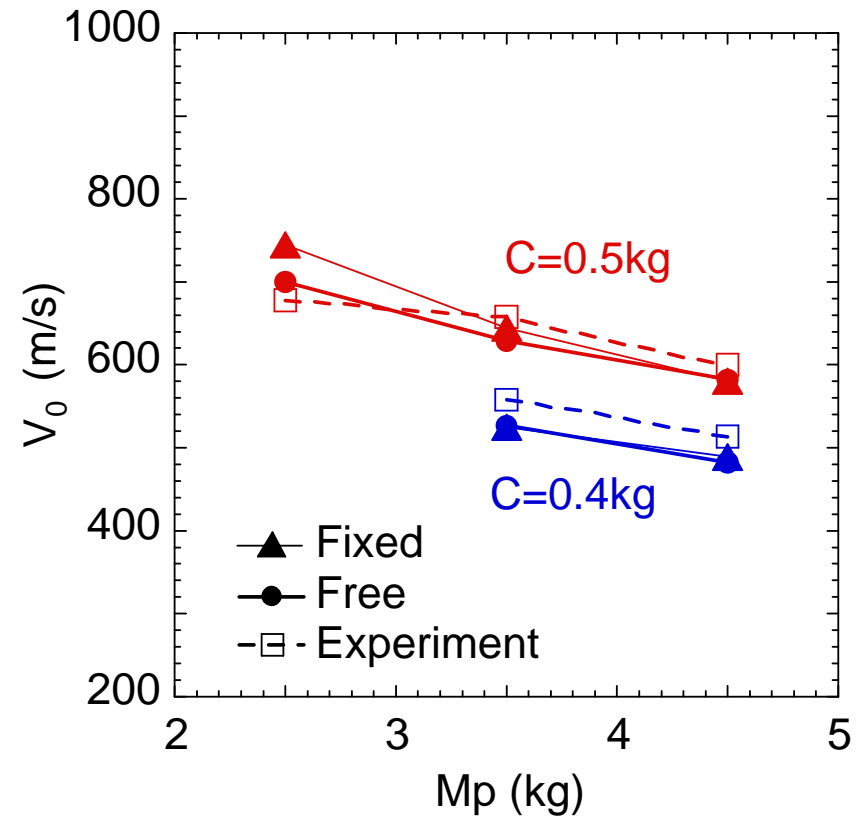
- ❑ If we use the fixed propellant model (without propellant movement), the predicted pressure becomes much higher than the free propellant model (with propellant movement).

and Fixed Propellant Models

Maximum Breech Pressure



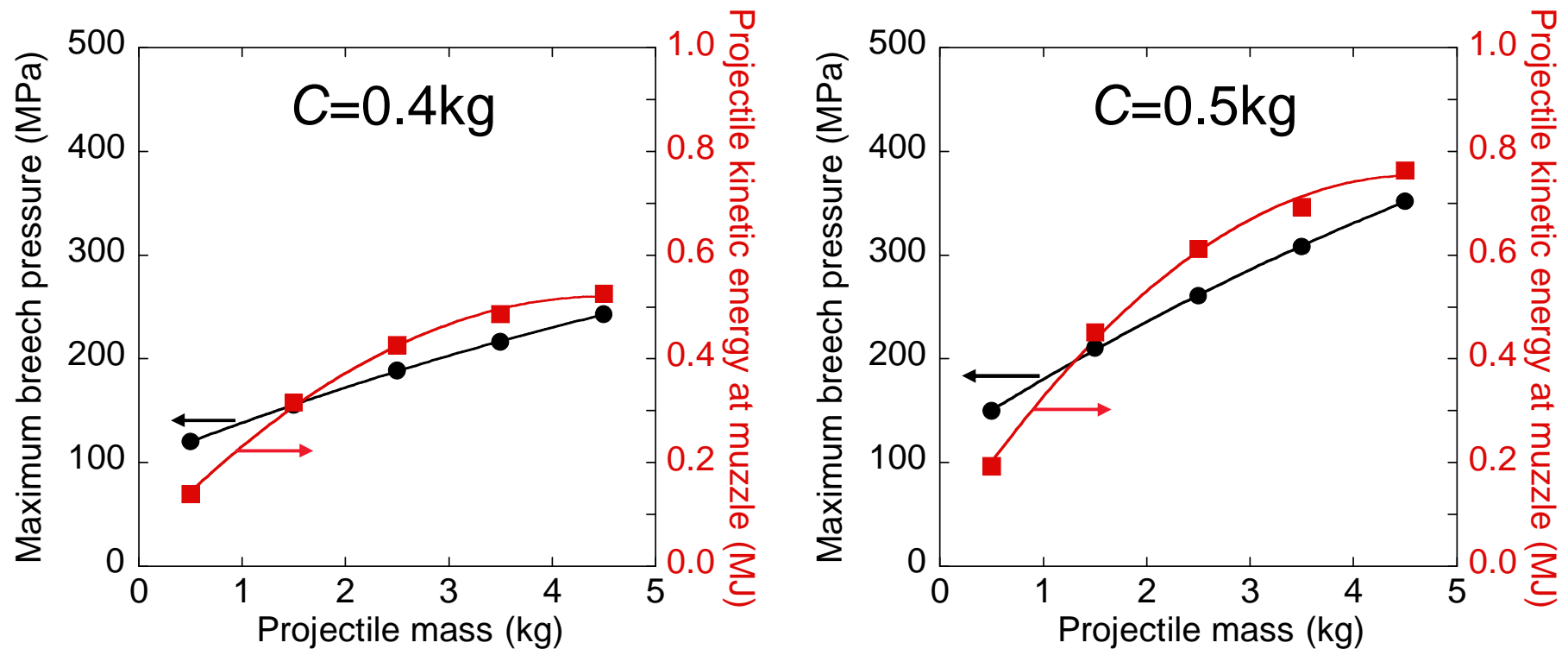
Muzzle Velocity



- ❑ The muzzle velocities of the two models were almost equivalent. However, the maximum breech pressure was overestimated by the **Fixed Model**, and the **Free Model** well reproduced the experimental maximum pressure.

ation of Projectile Mass

Simulated maximum breech pressure
and projectile kinetic energy



- ❑ The maximum chamber pressure increases linearly whereas the projectile kinetic energy converges with the projectile mass M_p .

Conclusion

The processes of accelerating a projectile by tubular solid propellant combustion in the 50mm projectile launch system were simulated for various cases using the developed 2D two-phase flow code and the moving overlapped grid method.

- ☐ In the comparison between the predicted results and the experimental data of various M_p and C condition, the results of the simulation with propellant movement showed being in good agreement with the experimental results.
- ☐ There was trade-off relation between the chamber pressure suppression and the projectile kinetic energy improvement. However, the projectile kinetic energy at the muzzle converged with increasing the projectile mass M_p .

Hiroaki MIURA

Belongs to Department of Mechanical Engineering
at Keio University in Japan

miura@mech.keio.ac.jp

dr074673@hc.cc.keio.ac.jp